

Characterizing Low-temperature Aqueous Alteration of Mars-Analog Basalts from Mauna Kea at Multiple Scales. B.P. Rasmussen¹, W.M. Calvin¹, B.L. Ehlmann², N. Lautze³, A.A. Fraeman⁴, T.S. Bristow⁵, J.W. DesOrmeau¹. ¹Department of Geological Sciences, University of Nevada, Reno, NV 89577 (brasmussen@nevada.unr.edu), ²Division of Geological and Planetary Sciences, California Institute of Technology, Pasadena, CA 91125, ³School of Ocean and Earth Science and Technology, University of Hawaii at Manoa, Honolulu, HI 96822, ⁴NASA Jet Propulsion Laboratory, Pasadena, CA 91109, ⁵NASA Ames Research Center, Moffett Field, CA 94035.

Introduction: Iron and magnesium rich phyllosilicates make up the large bulk of aqueous alteration mineralogy that has been identified on Mars [1]. However, the distribution of phyllosilicate phases raises many questions. Both dioctahedral and trioctahedral smectites have been observed on Mars, and current octahedral coordination provides a snapshot of the outcome of several possibilities during their formation and post-formation history. Trioctahedral, Fe²⁺ smectites are often found deep beneath layered aluminous clays that are thought to be the product of acid alteration and/or leaching more recently in Mars history [1,2]. Trioctahedral, Fe-Mg smectites are the thermodynamically-favored product of lower-temperature, anoxic aqueous alteration of basaltic material [3]. Dioctahedral, Fe³⁺ rich smectites are much more widespread and abundant in remotely sensed data. These Fe³⁺ rich smectites may have formed from prolonged oxidation of trioctahedral smectites which formed under anoxic conditions, or they may have formed directly under oxic conditions [4,5]. These varying formation conditions place very different constraints on Mars' atmospheric transitions and regional phenomena. Thus, due to the wide-reaching availability of CRISM and OMEGA spectral data, study of the variable VNIR (0.4-2.5 μm) spectral attributes of saponite and geologically realistic mixtures with common primary mafic minerals and other associated secondary minerals such as zeolites is important for Mars exploration.

Recent work has shown strong correlation between mineral phases identified via VNIR spectroscopy and more traditional methods such as X-ray diffraction (XRD), optical microscopy, and geochemical analyses [6]. More recent studies also show the utility of examining spatial relationships through spectral imaging and comparing spectral data with compositional information from scanning electron microscopy (SEM) [7,8]. Our analysis contributes a unique study of alteration of basalts in a subsurface environment and ties together multiple methods to observe small-scale and large-scale distributions, macro and microscopic textural information, and mineral associations as a Mars analog. It then ties the

interpretations back to VNIR absorption features to allow for broad applicability to other studies with the fast, non-destructive method of VNIR spectroscopy.

We performed a multi-scale characterization of aqueous alteration of Mars analog basaltic rock from the interior of Mauna Kea using high resolution VNIR spectral imaging, scanning electron microscopy, X-ray diffraction, and point VNIR spectra. The occurrence and distribution of several mineral classes and mineral assemblages have been identified in the high resolution data and cross-validated with multiple methods. Several assemblages of smectites and zeolites were identified. These mineral classes were mapped in cut sections extracted to represent the range of alteration products seen in the core samples and then spectral endmembers were used to map the field-collected point spectral data over nearly 1000m of depth.

Core Samples: In 2007 magnetotelluric surveys conducted across the Saddle Road on Mauna Kea in Hawaii indicated the presence of high elevation groundwater over broad regions [9]. In 2013 the Army Garrison and Office of Naval Research supported drilling a continuously-cored test hole over one conductive feature to define the local hydrologic conditions. The hole was drilled from March to June of 2013.

During drilling, a sequence of shallow perched aquifers at local-ambient temperatures were encountered, but were underlain by the regional water table showing considerably higher temperatures that increased with depth. At the bottom of the hole temperatures exceeded 140°C and the lower 700 m of the hole showed a temperature gradient of ~165°C/km. Deeper rocks showed progressive secondary mineralization with depth that was dominated by phyllosilicate and zeolite deposition. Fluid chemistry at 300 m depth in the regional aquifer was generally dilute and the Na-K and Na-K-Ca geothermometers yielded apparent equilibrium temperatures in the range of 250°C to 260°C [9].

Data Collection and Methods: Using an Analytical Spectral Devices (ASD) field spectrometer, we collected 780 spectra over the core depth interval from 3190' to 5785' (972 to 1763 m) over 3 days of

field work in May 2014. This device has a contact probe that integrates over a circular area ~ 10 mm in diameter and uses an internal halogen light source to measure reflected light over wavelengths from 0.4 to 2.5 μm at 5-7 nm spectral resolution. These spectra were used to determine eight alteration classes, which were mapped to depths using methods including a matched filter (MF), spectral angle map (SAM), and various color combinations and decorrelation stretch (DCS) products focused on specific mineral absorption features as described by [6].

This initial mapping guided cut-section extraction, where 25 samples were extracted for further analysis. Petrographic analysis guided a further reduction of samples to 8, which were imaged at high resolution (ultimately 240 μm pixels at 10 nm spectral resolution) in the VNIR, and examined with scanning electron microscopy. The remaining samples had bulk XRD analyses performed.

Spectral imaging, scanning electron microscopy, and details from XRD were used in combination to narrow down endmembers identified via the initial ASD field survey to single mineral or mineral groups of both primary and alteration minerals. These endmembers were then mapped in the VNIR spectral images using spectral feature fitting to observe small scale spatial relationships, while linear unmixing of the ASD spectra provided relative abundances of single minerals correlated with depth.

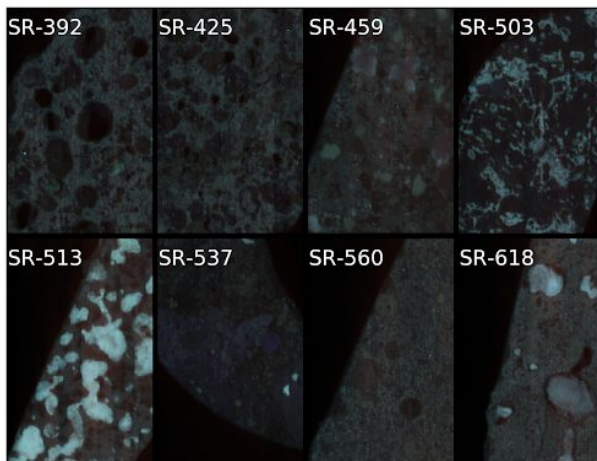


Figure 1: Mosaiced true color images of all samples inspected with VNIR imaging, SEM, and the ASD.

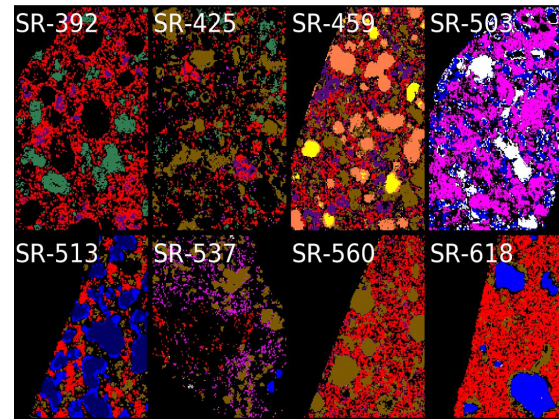


Figure 2: Mosaiced endmember classification results for the 8 high resolution spectral images.



Results: Trioctahedral Fe and Mg rich smectites were present but poorly crystalline towards the top of the zone of analysis (972 m), increasing in both crystallinity and abundance towards the bottom of sampling (1763 m). The general trend of the hole from top to bottom is less-altered to more altered, with weaker phyllosilicate alteration at the top, several zones of mixed zeolites towards the center, followed by crystalline saponite in the lowest sections. Distinctly absent are Fe-Mg phyllosilicates other than smectites, as well as carbonates, sulfates, and Al phyllosilicates such as kaolinite or illite. The suite of assemblages points to low to moderate temperature ($<250^\circ\text{C}$) alteration at neutral to basic pH in anoxic conditions, with little evidence of extensive surface interaction, presenting a useful terrestrial analog for an early Mars subsurface, anoxic environment. Stratigraphic control of alteration phases is likely controlled by slight fluctuations in pH. We also present a library of VNIR ASD spectra of the analyzed cut sections as a reference for use in future work.

References: [1] Ehlmann B. L. and Edwards C.S. (2014) *Ann. Rev. of EaPS*, 42, 291-315. [2] Bridges J. (2014) *AmMin*, 99 (11-12) 2163:2164. [3] Catalano J.G. (2013) *JGR*, 118 (10), 2124-2136. [4] Chemtob S.M. et al. (2017) *JGR*, 122 (12), 2469-2488. [5] Chemtob S.M. et al. (2015) *JGR*, 120 (6), 1119-1140. [6] Calvin W.M. and Pace E.L. (2016) *Geothermics*, 61, 12-23. [7] Greenberger R.N. et al. (2015) *GSA Today*, 25, 12, 4-10. [8] Leask E.K. and Ehlmann B.L. (2016) *WHISPERS 2016*, 17261833. [9] Thomas D.M. et al. (2014) *AGU 2014*, Abstract V21A-4731.